Hyperhoneycomb Iridate β-Li_2IrO_3 as a Platform for Kitaev Magnetism

T. Takayama,[1,2] A. Kato,[2] R. Dinnebier,[1] J. Nuss,[1] H. Kono,[2] L. S. I. Veiga,[3,4,5] G. Fabbris,[5,6] D. Haskel,[5] and H. Takagi[1,2]

[1]*Max Planck Institute for Solid State Research, Heisenbergstrasse 1, 70569 Stuttgart, Germany*
[2]*Department of Physics and Department of Advanced Materials, University of Tokyo, 7-3-1 Hongo, Tokyo 113-0033, Japan*
[3]*Instituto de Física "Gleb Wataghin", Universidade Estadual de Campinas, Campinas, São Paulo 13083-859, Brazil*
[4]*Laboratório Nacional de Luz Síncrotron, Campinas, São Paulo 13083-970, Brazil*
[5]*Advanced Photon Source, Argonne National Laboratory, Argonne, Illinois 60439, USA*
[6]*Department of Physics, Washington University, St. Louis, Missouri 63130, USA*

(Received 11 September 2014; published 19 February 2015)

A complex iridium oxide β-Li_2IrO_3 crystallizes in a hyperhoneycomb structure, a three-dimensional analogue of honeycomb lattice, and is found to be a spin-orbital Mott insulator with $J_{\rm eff} = 1/2$ moment. Ir ions are connected to the three neighboring Ir ions via Ir-O_2-Ir bonding planes, which very likely gives rise to bond-dependent ferromagnetic interactions between the $J_{\rm eff} = 1/2$ moments, an essential ingredient of Kitaev model with a spin liquid ground state. Dominant ferromagnetic interaction between $J_{\rm eff} = 1/2$ moments is indeed confirmed by the temperature dependence of magnetic susceptibility $\chi(T)$ which shows a positive Curie-Weiss temperature $\theta_{\rm CW} \sim +40$ K. A magnetic ordering with a very small entropy change, likely associated with a noncollinear arrangement of $J_{\rm eff} = 1/2$ moments, is observed at $T_c = 38$ K. With the application of magnetic field to the ordered state, a large moment of more than 0.35 μ_B/Ir is induced above 3 T, a substantially polarized $J_{\rm eff} = 1/2$ state. We argue that the close proximity to ferromagnetism and the presence of large fluctuations evidence that the ground state of hyperhoneycomb β-Li_2IrO_3 is located in close proximity of a Kitaev spin liquid.

DOI: 10.1103/PhysRevLett.114.077202 PACS numbers: 75.10.Kt, 75.70.Tj, 75.25.Dk

The recent surge of interest in the physics of spin-orbit coupling (SOC) in $5d$ transition-metal based oxides was initiated by the discovery of a spin-orbital Mott insulating state in the layered iridate Sr_2IrO_4 [1]. In Sr_2IrO_4, Ir^{4+} ions with five $5d$ electrons are octahedrally coordinated with O^{2-} ions. The large splitting between the t_{2g} and e_g manifolds, due to cubic crystal field, allocates all five electrons into the t_{2g} manifold. SOC of heavy Ir, as large as 0.6 eV, reconstructs the t_{2g} manifold into a lower filled $J_{\rm eff} = 3/2$ quartet and upper half-filled $J_{\rm eff} = 1/2$ doublet. The $J_{\rm eff} = 1/2$ state consists of equal superposition of three t_{2g} orbitals with real and imaginary orbital components and opposite spins, $|J_{\rm eff} = 1/2\rangle = (1/\sqrt{3})[|d_{xy}, \pm\sigma\rangle \pm |d_{yz}, \mp\sigma\rangle + i|d_{zx}, \mp\sigma\rangle]$, where σ denotes the spin state. Localized $J_{\rm eff} = 1/2$ moments are produced by the presence of modest Coulomb U in the half-filled $J_{\rm eff} = 1/2$ band, giving rise to a novel spin-orbital Mott insulator. The $J_{\rm eff} = 1/2$ Mott state has been established in a number of complex Ir^{4+} oxides [2–4].

One of the most intriguing outcomes unique to the $J_{\rm eff} = 1/2$ Mott state may be an exotic magnetic coupling derived from the imaginary component of the $J_{\rm eff} = 1/2$ wave function [5]. In the edge-shared configuration of two adjacent IrO_6 octahedra, $J_{\rm eff} = 1/2$ moments interact essentially via the two 90° Ir-O-Ir bonds forming a square Ir-O_2-Ir plane. The presence of imaginary components in the wave function yields a destructive interference of superexchange paths between the two Ir-O-Ir bonds. The remnant magnetic interaction, stemming from Hund's coupling, has a form of *bond-dependent ferromagnetic interaction*, which is an essential ingredient of the Kitaev model [6]. The Kitaev model consists of bond-dependent anisotropic and ferromagnetic coupling between the neighboring spins on a honeycomb lattice. If the three bonds sharing the same spin have ferromagnetic coupling only for x, y, and z components, respectively, the bond-dependent polarization of spins conflicts with each other, giving rise to a frustration. The ground state of the Kitaev model with such bond frustration was solved exactly, and known to be a quantum spin liquid. The solid-state platform for the model, however, has been elusive so far. The honeycomb iridates comprising edge-sharing IrO_6 octahedra thus appear to be a promising arena for its materialization.

Possible realization of the Kitaev model in the honeycomb iridates α-Li_2IrO_3 and α-Na_2IrO_3 has triggered intensive investigations both experimentally and theoretically. Both α-Li_2IrO_3 and α-Na_2IrO_3 were discovered to order antiferromagnetically at around 15 K [7–9]. The Curie Weiss temperature is negative, ~ -125 K for Na_2IrO_3 and ~ -40 K for Li_2IrO_3. This means that antiferromagnetic interaction, stronger than the ferromagnetic superexchange coupling, is present [10]. The magnetic ordering of Na_2IrO_3 was found to be a zigzag type [11,12]. This could be ascribed to the coexistence of a Kitaev-type ferromagnetic interaction with dominant antiferromagnetic interactions [13,14]. The weak signature of the Kitaev interaction posed a serious question as to whether it is possible to approach the Kitaev limit in honeycomb α-Na_2IrO_3 and α-Li_2IrO_3.

The two honeycomb iridates have been so far the sole playground for the realization of the Kitaev model. In the search for a new platform for Kitaev physics, we discovered a new form of Li_2IrO_3, β-Li_2IrO_3, consisting of a three-dimensional analogue of the honeycomb lattice of Ir^{4+} ions which we call the "hyperhoneycomb" lattice. The magnetic susceptibility $\chi(T)$ of β-Li_2IrO_3 evidences the dominant ferromagnetic coupling, very likely representing the Kitaev-type interaction. A noncollinear magnetic ordering is observed at 38 K, which turns into a ferromagnetic state of $J_{\rm eff} = 1/2$ moments under magnetic fields above 3 T. Theoretical studies on an extended Kitaev model for a hyperhoneycomb lattice demonstrated that the ground state should be also a quantum spin liquid [15]. We argue that the above results place β-Li_2IrO_3 in close proximity to the three-dimensional Kitaev spin liquid.

The polycrystalline samples of β-Li_2IrO_3 were synthesized by a solid state reaction from Li_2CO_3, IrO_2 and LiCl in a molar ratio of 10 : 1 : 100. The mixture was pressed into a pellet, and heated at 1100 °C for 24 h, cooled to 700 °C at a rate of 30 K/h and furnace cooled to room temperature. The sample was rinsed with distilled water to remove excess LiCl. The obtained powder product was found to consist of a new phase and a small trace of IrO_2 from the powder x-ray diffraction pattern [16]. The new phase was revealed to be a new form of Li_2IrO_3, β-Li_2IrO_3, isostructural to β-Na_2PtO_3 [23]. The detailed structure was then refined by single crystal x-ray analysis using 50 μm-size crystal grains. The result of the refinement is summarized in Table I.

The crystal structure of β-Li_2IrO_3 is illustrated in Fig. 1(a). It can be described as a distorted cubic close packed arrangement of oxygen atoms with iridium and lithium atoms occupying all octahedral holes in a specific ordered manner. The local structure around an iridium atom is closely related to that of honeycomb α-Li_2IrO_3. Each IrO_6 octahedron is connected with three neighboring IrO_6 octahedra by sharing its three edges [Fig. 1(b)], which gives rise to three Ir-O_2-Ir planar bonds with their planes almost orthogonal to each other. When Ir ions have a $J_{\rm eff} = 1/2$ moment, the exchange interaction via Ir-O_2-Ir paths very likely gives rise to anisotropic ferromagnetic coupling [5]. The network of iridium ions in β-Li_2IrO_3, depicted in Fig. 1(c), is closely linked to a honeycomb lattice. The 2D honeycomb lattice can be viewed as planar zigzag chains connected at the corners with bridging bonds. In the Ir sublattice of β-Li_2IrO_3, the zigzag Ir chains are connected by the bridging bonds parallel to the c axis. In contrast to the 2D honeycomb lattice, however, the zigzag chains are alternately rotated by 69.9° about the c axis [pink and blue chains in Fig. 1(c)] and connected to the bridging bonds in the layers above and below. Because of the close link to honeycomb structure, the Ir sublattice in β-Li_2IrO_3 may be called hyperhoneycomb. In the hyperhoneycomb Ir sublattice, all the angles between the three Ir-Ir bonds are very close to 120°, and the distances between Ir atoms are almost equivalent (only ~0.2% difference).

As an extension of the Kitaev model, the lattice equivalent to hyperhoneycomb lattice, with competing ferromagnetic polarizations between the three bonds, was studied theoretically [15]. The model could be mapped onto the Kitaev model and is exactly solvable. The ground state is a spin-liquid state as in the original Kitaev model.

TABLE I. Structural parameters of β-Li_2IrO_3. The space group is $Fddd$ (No. 70) and $Z = 16$, and the lattice constants are $a = 5.9104(3)$ Å, $b = 8.4562(4)$ Å, and $c = 17.8271(9)$ Å. g and $U_{\rm iso}$ denote site occupancy and the isotropic displacement parameter, respectively. The final R indices are $R = 0.027$ and $wR = 0.0480$.

Atom	Site	g	x	y	z	$U_{\rm iso}$(Å^2)
Ir	16g	1	1/8	1/8	0.70854(2)	0.00560(4)
O(1)	16e	1	0.8572(5)	1/8	1/8	0.0078(4)
O(2)	32h	1	0.6311(5)	0.3642(3)	0.0383(1)	0.0094(3)
Li(1)	16g	1	1/8	1/8	0.0498(5)	0.0051(11)
Li(2)	16g	1	1/8	1/8	0.8695(7)	0.0155(18)

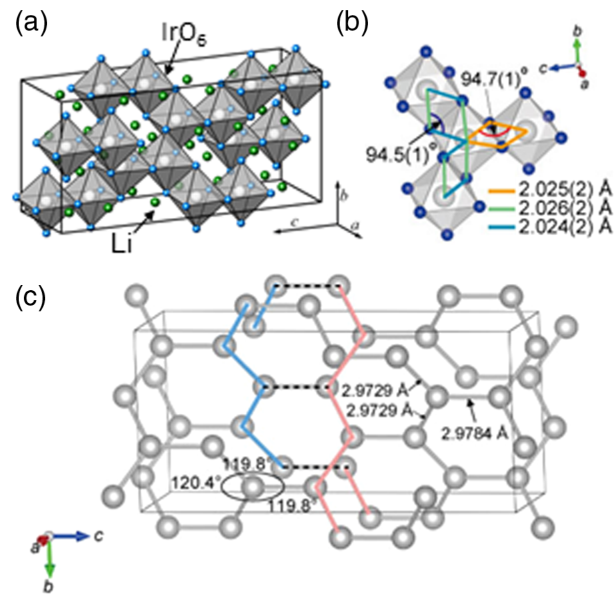

FIG. 1 (color online). (a) Crystal structure of β-Li_2IrO_3. Green, gray, and blue spheres represent lithium, iridium, and oxygen atoms, respectively. (b) Local lattice network of IrO_6 octahedra in β-Li_2IrO_3 [24], displaying Ir-O bond lengths and two different Ir-O-Ir angles obtained from the single crystal analysis [16]. (c) Hyperhoneycomb lattice of Ir ions in β-Li_2IrO_3. The pink and blue lines show the twisted zigzag chains alternating along the c axis. The black dotted lines are the bond bridging the zigzag chains. The numbers indicated are Ir-Ir distances and the angles between Ir atoms.

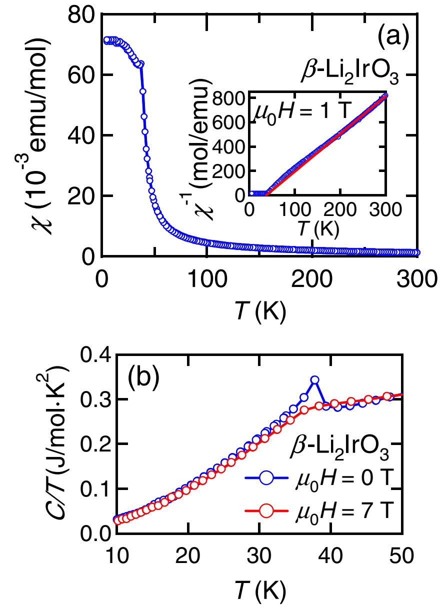

FIG. 2 (color online). (a) Temperature dependence of magnetic susceptibility for β-Li_2IrO_3 under 1 T. The inset shows the temperature dependence of the inverse of magnetic susceptibility. The red solid line delineates the Curie-Weiss fit at high temperatures between 200 and 350 K. (b) Temperature dependence of specific heat divided by temperature recorded at 0 and 7 T.

We may therefore anticipate Kitaev physics and a possible spin-liquid state in β-Li_2IrO_3.

Resistivity measurements indicate that β-Li_2IrO_3 is an insulator with a magnitude of resistivity of the order of $100\ \Omega\,\mathrm{cm}$ at room temperature, which is 1 order of magnitude larger than that of α-Li_2IrO_3 [9]. Combined with the presence of the $J_{\mathrm{eff}} = 1/2$ moments described below, we conclude that β-Li_2IrO_3 is a spin-orbital Mott insulator as in α-Li_2IrO_3. The temperature dependence of magnetic susceptibility $\chi(T)$, measured on the polycrystalline sample, is shown in Fig. 2(a). The Curie-Weiss fitting at high temperatures between 200 and 350 K yields an effective moment of 1.61 μ_B/Ir, close to 1.73 μ_B/Ir of the ideal $J_{\mathrm{eff}} = 1/2$ moment, and a positive Curie-Weiss temperature $\theta_{\mathrm{CW}} \sim +40$ K. These imply the formation of $J_{\mathrm{eff}} = 1/2$ moments and the dominant ferromagnetic interaction among them. With decreasing temperature, $\chi(T)$ shows a steep increase below ~50 K, followed by a sharp kneelike anomaly at $T_c = 38$ K indicative of magnetic ordering. The specific heat $C(T)$ shows an anomaly at $T_c = 38$ K, evidencing a second order magnetic phase transition. $\chi(T)$ does not show a decrease below T_c, in contrast to those of collinear antiferromagnets. The ground state therefore is very likely a noncollinear antiferromagnet.

The Curie-Weiss temperature $\theta_{\mathrm{CW}} \sim +40$ K is very close to $T_c = 38$ K, which at a glance would suggest a mean field like transition. Contrary to this, however, the magnetic entropy associated with the transition, estimated as ~0.2 J/mol K from the specific heat anomaly, is at most

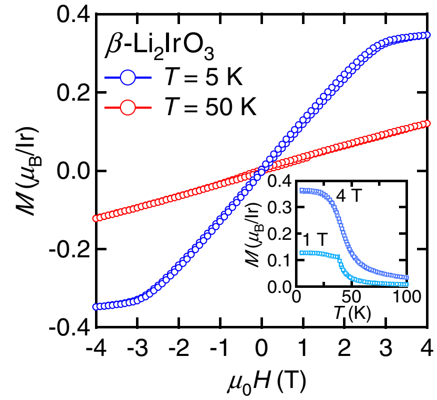

FIG. 3 (color online). Magnetization curve of β-Li_2IrO_3. The blue and red dots are data taken at 5 and 50 K, respectively. The inset shows the temperature dependence of magnetization under a magnetic field of 1 and 4 T.

a few % of $R \ln 2$, indicative of the presence of strong fluctuations. $\theta_{\mathrm{CW}} \sim +40$ K is therefore very likely a consequence of cancellation of ferromagnetic and antiferromagnetic interactions and the actual energy scale of ferromagnetic interactions should be much larger than that estimated from θ_{CW}. This can be reasonably understood as the dominance of bond-dependent ferromagnetic interaction over other antiferromagnetic ones [25]. Frustrations must be involved in the magnetism and the magnetic ordering at $T_c = 38$ K is marginally achieved [26].

The ground state is very close to ferromagnetism. The magnetization curve at 5 K (Fig. 3) clearly shows a magnetic-field induced change to a ferromagnetic state. At low fields, the magnetization increases linearly with field. With further increasing field, a kink is observed at $\mu_0 H_c \sim 3$ T, followed by a gradual increase above 3 T. The magnitude of magnetization above 3 T is remarkably large, ~$0.35\,\mu_B$/Ir, which is in marked contrast to the weak ferromagnetism with a moment of $0.07\,\mu_B$/Ir arising from the canted $J_{\mathrm{eff}} = 1/2$ moments in Sr_2IrO_4 [1]. The ordered moment in other antiferromagnetic iridates such as Sr_2IrO_4 and α-Na_2IrO_3 was reported to be around 0.20–0.36 μ_B/Ir [27,28] and 0.22 μ_B/Ir [12], respectively. The large induced magnetization above $0.35\,\mu_B$/Ir cannot be attributed to canting of $J_{\mathrm{eff}} = 1/2$ moments, implying that the $J_{\mathrm{eff}} = 1/2$ moments in β-Li_2IrO_3 are about being fully polarized above 3 T. We argue that the kink at $\mu_0 H_c \sim 3$ T may represent the lowest saturation field of $J_{\mathrm{eff}} = 1/2$ moments in the magnetization measurement on a polycrystalline sample with randomly oriented grains. The torque measurements on a small single crystal grain in fact indicated the presence of magnetic anisotropy [29]. Under a magnetic field of 4 T, the cusp at 38 K seen in the low field $M(T)$ fades out as shown in the inset of Fig. 3. In accord with this, the peak in C/T is smeared out above 3 T, consistent with a ferromagnetic state of $J_{\mathrm{eff}} = 1/2$ moments in the field.

The proximity to a ferromagnetic state, as well as the presence of strong fluctuations, indicates that

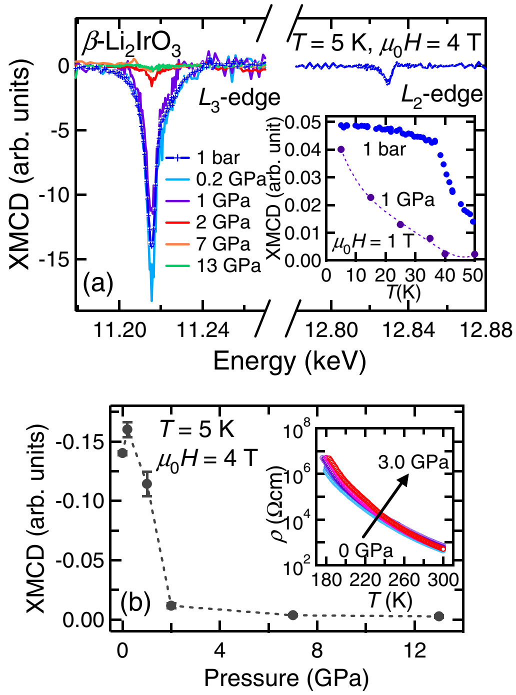

FIG. 4 (color online). (a) XMCD spectra at the Ir $L_{2,3}$ edges for β-Li_2IrO_3. The data are collected at $T = 5$ K, $\mu_0 H = 4$ T. The spectra at the L_3 edge were also measured under high pressures. The inset shows the temperature dependence of the XMCD signal measure at 1 T under ambient pressure and 1–1.5 GPa. The uncertainty of pressure derives from the pressure change with temperature. (b) Pressure dependence of the XMCD signal of the L_3 edge at $T = 5$ K, $\mu_0 H = 4$ T. The inset shows the temperature dependence of resistivity measured at 0, 0.3, 0.9, 1.2, 1.8, 2.4, and 3.0 GPa.

hyperhoneycomb β-Li_2IrO_3 is located at much closer vicinity to the Kitaev spin liquid than α-Na_2IrO_3 and α-Li_2IrO_3. In those honeycomb iridates the weak signature of Kitaev-type interaction was at least partly ascribed to the distortion of planar Ir-O_2-Ir bonds [9,30]. The Ir-O-Ir angles of ~95° for α-Li_2IrO_3 [7] and ~98° for α-Na_2IrO_3 [31] deviate appreciably from the ideal value of 90°. The two Ir-O bonds forming the Ir-O_2-Ir plane are not equivalent, ~5.7% different in length for α-Li_2IrO_3 [7]. In sharp contrast, in β-Li_2IrO_3, the Ir-O-Ir angles are ~94.5° and the difference in the length among the inequivalent Ir-O bonds is only ~0.2%, orders of magnitude smaller than that of α-Li_2IrO_3.

The nature of field-induced moments in the ordered state was investigated by x-ray magnetic circular dichroism (XMCD) on polycrystalline samples [16]. XMCD enables us to separate the spin and the orbital contributions to the magnetic moments. The XMCD spectra at 4 T shown in Fig. 4(a) display a clear asymmetry between the L_3 (13% dichroism) and L_2 (1.4% dichroism) edges, similar to those observed in other iridates [32,33]. Assuming $\langle n_h \rangle = 5$ for the number of 5d holes, the net orbital moment is estimated to be $M_L = 0.242\,\mu_B$/Ir from the orbital sum rule for XMCD [34]. The magnitude of magnetization M_{total} measured at 4 T, ~$0.35\,\mu_B$/Ir, yields the net spin moment $M_S = M_{\mathrm{total}} - M_L = 0.35 - 0.242 \sim 0.11\ \mu_B$/Ir. The ratio of the orbital and the spin moments $\langle L_z \rangle / \langle S_z \rangle$ is therefore ~4.4, which is very close to 4, expected for the ideal $J_{\mathrm{eff}} = 1/2$ moments [35]. The $J_{\mathrm{eff}} = 1/2$ picture works very well in β-Li_2IrO_3.

The magnetic-field-induced ferromagnetic moments were found to be suppressed rapidly by applying pressure. As shown in Figs. 4(a) and 4(b), the XMCD signal starts to decrease above a pressure of 1 GPa accompanied by the strongly broadened transition, and almost vanishes above 2 GPa. The resistivity data shown in the inset of Fig. 4(b) indicate that β-Li_2IrO_3 remains insulating above 2 GPa. This implies that the vanishing of the XMCD signal is due to the rearrangement of $J_{\mathrm{eff}} = 1/2$ moments rather than the disappearance of localized $J_{\mathrm{eff}} = 1/2$ moments, suggesting the presence of energetically almost degenerate states near the ground state.

We argue that the small structural distortion of Ir-O_2-Ir bonds and the almost ideal $J_{\mathrm{eff}} = 1/2$ local wave function in β-Li_2IrO_3 result in the predominance of Kitaev-type ferromagnetic interaction over the other interactions, including the nearest-neighbor Heisenberg and the long-range interactions. The other interactions, however, are not zero and superposed onto Kitaev-type ferromagnetic interaction, which we argue stabilize marginally the noncollinear ordering below $T_c = 38$ K. The noncollinear spiral order is indeed envisaged to manifest itself at the critical boundary to the Kitaev liquid in the theoretical phase diagram of the extended Kitaev-Heisenberg model for 2D honeycomb lattice [36] and also for 3D analogues [37]. Under pressure, the intricate balance between Kitaev-type and other interactions is modified, resulting in a different magnetic ground state.

In summary, a complex Ir^{4+} oxide, β-Li_2IrO_3, crystallizes in an intriguing structure, the hyperhoneycomb, which is a three-dimensional analogue of two-dimensional honeycomb structure. $J_{\mathrm{eff}} = 1/2$ moments on the hyperhoneycomb lattice, connected by the planar Ir-O_2-Ir bonds, provide a promising playground towards the realization of Kitaev spin liquid. The magnetization data clearly support the predominance of Kitaev-type ferromagnetic interaction and the close proximity of β-Li_2IrO_3 to the Kitaev spin liquid state. However, the presence of other interactions, small but finite, appears to stabilize marginally a noncollinear ordering below $T_c = 38$ K. Those results suggest that β-Li_2IrO_3 be the most promising candidate for the long-sought Kitaev spin liquid to date.

We thank A. W. Rost for invaluable discussions and critical reading of the manuscript. We are grateful to B. J. Kim, A. Jain, L. Hozoi, and G. Jackeli for fruitful discussion. This work was partly supported by Grant-in-Aid for Scientific Research (S) (Grant No. 24224010). Work at Argonne was supported by the U.S. Department of

Energy, Office of Science, under Contract No. DE-AC02-06CH11357. L. S. I. Veiga is supported by FAPESP (SP-Brazil) under Contract No. 2013/14338-3.

[1] B. J. Kim, H. Ohsumi, T. Komesu, S. Sakai, T. Morita, H. Takagi, and T. Arima, Science **323**, 1329 (2009).
[2] S. Fujiyama, K. Ohashi, H. Ohsumi, K. Sugimoto, T. Takayama, T. Komesu, M. Takata, T. Arima, and H. Takagi Phys. Rev. B **86**, 174414 (2012).
[3] K. Ohgushi, J.-i. Yamaura, H. Ohsumi, K. Sugimoto, S. Takeshita, A. Tokuda, H. Takagi, M. Takata, and T.-h. Arima, Phys. Rev. Lett. **110**, 217212 (2013).
[4] S. Boseggia, R. Springell, H. Walker, H. Rønnow, Ch. Rüegg, H. Okabe, M. Isobe, R. Perry, S. Collins, and D. McMorrow, Phys. Rev. Lett. **110**, 117207 (2013).
[5] G. Jackeli and G. Khaliullin, Phys. Rev. Lett. **102**, 017205 (2009).
[6] A. Kitaev, Ann. Phys. (Amsterdam) **321**, 2 (2006).
[7] M. J. O'Malley, H. Verweij, and P. M. Woodward, J. Solid State Chem. **181**, 1803 (2008).
[8] Y. Singh and P. Gegenwart, Phys. Rev. B **82**, 064412 (2010).
[9] Y. Singh, S. Manni, J. Reuther, T. Berlijn, R. Thomale, W. Ku, S. Trebst, and P. Gegenwart, Phys. Rev. Lett. **108**, 127203 (2012).
[10] J. Chaloupka, G. Jackeli, and G. Khaliullin, Phys. Rev. Lett. **105**, 027204 (2010).
[11] X. Liu, T. Berlijn, W.-G. Yin, W. Ku, A. Tsvelik, Y.-J. Kim, H. Gretarsson, Y. Singh, P. Gegenwart, and J. P. Hill, Phys. Rev. B **83**, 220403(R) (2011).
[12] F. Ye, S. Chi, H. Cao, B. C. Chakoumakos, J. A. Fernandez-Baca, R. Custelcean, T. F. Qi, O. B. Korneta, and G. Cao, Phys. Rev. B **85**, 180403(R) (2012).
[13] I. Kimchi and Y. Z. You, Phys. Rev. B **84**, 180407(R) (2011).
[14] J. Chaloupka, G. Jackeli, and G. Khaliullin, Phys. Rev. Lett. **110**, 097204 (2013).
[15] S. Mandal and N. Surendran, Phys. Rev. B **79**, 024426 (2009).
[16] See Supplemental Material at http://link.aps.org/supplemental/10.1103/PhysRevLett.114.077202, which includes Ref. [17–22], for experimental details.
[17] A. Biffin, R. D. Johnson, S. Choi, F. Freund, S. Manni, A. Bombardi, P. Manuel, P. Gegenwart, and R. Coldea, Phys. Rev. B **90**, 205116 (2014).
[18] Bruker Suite, Version 2013/10, Bruker AXS Inc., Madison, USA (2013).
[19] G. M. Sheldrick, SADABS—Bruker AXS area detector scaling and absorption, version 2012/1, University of Göttingen, Germany (2012).
[20] G. M. Sheldrick, Acta Crystallogr. Sect. A **64**, 112 (2008).
[21] Further details may be obtained from Fachinformations-zentrum Karlsruhe, 76344 Eggenstein-Leopoldshafen, Germany [fax: (+49)-7247-808-666; e-mail: crysdata(at) fiz-karlsruhe.de, http://www.fiz-karlsruhe.de/request_for_deposited_data.html] on quoting the CSD number (427415).
[22] C. T. Chen, Y. Idzerda, H.-J. Lin, N. Smith, G. Meigs, E. Chaban, G. Ho, E. Pellegrin, and F. Sette, Phys. Rev. Lett. **75**, 152 (1995).
[23] W. Urland and R. Hoppe, Z. Anorg. Allg. Chem. **392**, 23 (1972).
[24] K. Momma and F. Izumi, J. Appl. Crystallogr. **44**, 1272 (2011).
[25] J. Reuther, R. Thomale, and S. Trebst, Phys. Rev. B **84**, 100406(R) (2011).
[26] Note that the ordering temperature does not necessarily scale with the Curie-Weiss temperature when the ferromagnetic Kitaev and other antiferromagnetic interactions coexist. The coincidence of the Curie-Weiss temperature and the ordering temperature is likely accidental.
[27] F. Ye, S. Chi, B. C. Chakoumakos, J. A. Fernandez-Baca, T. Qi, and G. Cao, Phys. Rev. B **87**, 140406(R) (2013).
[28] C. Dhital, T. Hogan, Z. Yamani, C. de la Cruz, X. Chen, S. Khadka, Z. Ren, and S. Wilson, Phys. Rev. B **87**, 144405 (2013).
[29] A. W. Rost *et al.* (unpublished).
[30] S. Bhattacharjee, S. S. Lee, and Y. B. Kim, New J. Phys. **14**, 073015 (2012).
[31] S. K. Choi *et al.*, Phys. Rev. Lett. **108**, 127204 (2012).
[32] M. A. Laguna-Marco, D. Haskel, N. Souza-Neto, J. C. Lang, V. V. Krishnamurthy, S. Chikara, G. Cao, and M. van Veenendaal, Phys. Rev. Lett. **105**, 216407 (2010).
[33] D. Haskel, G. Fabbris, M. Zhernenkov, P. P. Kong, C. Q. Jin, G. Cao, and M. van Veenendaal, Phys. Rev. Lett. **109**, 027204 (2012).
[34] B. T. Thole, P. Carra, F. Sette, and G. van der Laan, Phys. Rev. Lett. **68**, 1943 (1992).
[35] In the cubic limit, $J_{\rm eff} = 1/2$ wave function yields $\langle L_z \rangle = 2/3$ and $\langle S_z \rangle = 1/6$ due to a mixture of up- and down-spin components, and thus the ratio $\langle L_z \rangle / \langle S_z \rangle$ is 4.
[36] J. G. Rau, E. K. H. Lee, and H. Y. Kee, Phys. Rev. Lett. **112**, 077204 (2014).
[37] E. K. H. Lee and Y. B. Kim, arXiv:1407.4125.